Localization of Mobile Robot by Particle Filter Considering Shape Information of Environment and Location of Water Puddles

Isao Tadokoro, Ryosuke Kataoka, Ryuki Suzuki, Yonghoon Ji, and Kazunori Umeda

***Abstract*— In this paper, we propose a method to estimate robot pose accurately by considering environmental features for the particle filter. Particle filters have been widely used for pose estimation of mobile robots. However, the accuracy of the self-positioning estimation is degraded in environments where the shape features are scarce. Therefore, a novel likelihood function is designed by taking into account the environmental features for the particle filter. We improve the accuracy of the pose estimation by fusing the likelihood of the shape information and the likelihood of the binary attribute information in the water puddle for the particle filter.**

I. INTRODUCTION

After the Great East Japan Earthquake on March 11, 2011, the Fukushima Daiichi Nuclear Power Station leaked radioactive materials, making it difficult for humans to enter the plant. Therefore, robots have been attracting attention for exploration and decommissioning activities in place of humans. In the operation of mobile robots, it is necessary to always know the robot pose and particle filters reflecting information from range sensor are commonly used [1-4]. However, these studies consider only the shape features of the environment, and pose estimation is difficult in environments with poor shape features. For example, long corridors. Ohno et al. proposed a method to identify valid GPS observations using odometry and to reflect the GPS information in a particle filter [5]. Nishimura et al. proposed a method to discriminate valid observations by recognizing obstacle areas and sky areas using an infrared camera to capture the sky above [6]. However, these studies cannot provide accurate pose estimation inside a nuclear reactor building because it is difficult to continuously input valid GPS observations indoors. Yamaguchi et al. proposed a method to improve the accuracy of pose estimation by recognizing white lines and road signs as landmarks by extracting edges from images captured with a fisheye camera and reflecting them in a particle filter [7]. However, it is difficult to improve pose estimation because white lines and road signs that serve as landmarks cannot be observed in the nuclear power plant. Hatakeyama et al. proposed a pose estimation method using range images obtained from a depth camera [8]. However, light in the reactor building after a disaster is insufficient for observation with a camera. Therefore, effective information cannot be obtained, making pose estimation difficult.

In this study, we use light detection and ranging (LiDAR), which is effective even in dark places, to observe the shape information of the environment. And, it is expected that a large number of water puddles exist in the damaged nuclear power plant. Then, we propose a method to improve the accuracy of pose estimation in a nuclear reactor building after a disaster by using a near-infrared sensor to observe the feature quantities of water puddle in the damaged nuclear power plant and reflecting them in a particle filter.

The remainder of this paper is as follows. Section II provides an overview of the proposed method. Simulation results are detailed in Section III. Finally, Section IV provides conclusions and insights on future work.

II. PROPOSED METHOD

A. *Overview of the Proposed Method*

Figure 1 shows a flowchart of the proposed method. In this study, the method proposed by Dellaert et al. is adopted as a reference method [1]. Particle Filter is a type of time series filtering, a method that can sequentially estimate future states from past states. The algorithm is roughly divided into four processes: "Prediction", "Update", "Resampling" and "Localization", which are repeated to estimate robot pose. In the proposed method, in addition to

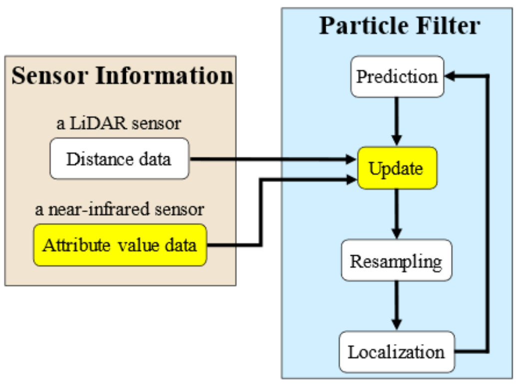

Figure 1. Flowchart of proposed framework.

Isao Tadokoro is with the Course of Precision Engineering, School of Science and Engineering, Chuo University, Tokyo, Japan (e-mail: tadokoro@sensor.mech.chuo-u.ac.jp).

Ryosuke Kataoka was with the Course of Precision Engineering, School of Science and Engineering, Chuo University, Tokyo, Japan (e-mail: kataoka@sensor.mech.chuo-u.ac.jp).

Ryuki Suzuki was with the Course of Precision Engineering, School of Science and Engineering, Chuo University, Tokyo, Japan (e-mail: suzuki@sensor.mech.chuo-u.ac.jp).

Yonghoon Ji is with Graduate School for Advanced Science and Technology, JAIST, Nomi, Japan (e-mail: ji-y@jaist.ac.jp).

Kazunori Umeda is with the Faculty of Precision Engineering, School of Science and Engineering, Chuo University, Tokyo, Japan (e-mail: umeda@mech.chuo-u.ac.jp).

2023 IEEE/SICE International Symposium on System Integration (SII) | 979-8-3503-9868-7/23/$31.00 ©2023 IEEE | DOI: 10.1109/SII55687.2023.10039364

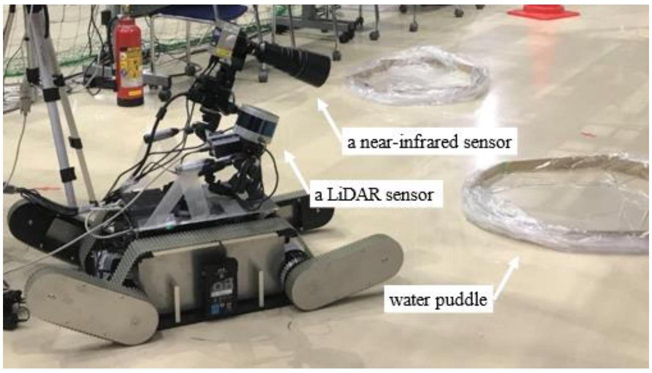

Figure 2. Sensor system.

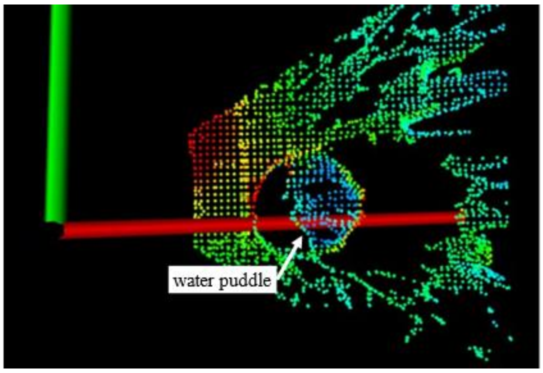

Figure 3. Point cloud of water puddle.

the distance value obtained from LiDAR, the "attribute" of water puddle obtained from a near-infrared sensor is added to the "Update" part. As shown in Figures 2 and 3, Kataoka et al. combined LiDAR with the sensor system in [9], and succeeded in obtaining point clouds of the intensity of LiDAR and the intensity of a near-infrared sensors [10]. In this research, we define "attribute value" as the presence or absence of environmental properties or features, specifically water puddles. The robot considered in this research is equipped with a LiDAR sensor and a near-infrared sensor, and that it is capable of obtaining distance values and attribute values for its surroundings. The attribute values are assumed to be obtained by observing water puddles.

B. *Observation Method*

To observe water puddles, we refer to Sugawara et al. [11]. They constructed a sensing system for three-dimensional (3D) visualization of the presence of water puddles, such as contaminated water leaks and water puddles in a nuclear power plant, and enables the measurement of the distance to the water puddles.

C. *Likelihood Calculation*

In this study, we assume that the measurements are made by the sensor system described in section II-A, and that the measured values for each laser of LiDAR include distance value and binary attribute value. In the weighting of each particle in the particle filter, the likelihood function $g(p, \mu)$ for the distance value of one laser of LiDAR is shown in the following equation:

$$g(p,\mu) = \frac{1}{\sqrt{2\pi\sigma_g^2}} exp\left\{-\frac{(p-\mu)^2}{2\sigma_g^2}\right\} \tag{1}$$

where μ and p are the distance value actually measured and the distance value obtained by ray tracing from each particle's posture using map information, respectively. σ_g^2 is the variance of the error of the distance value.

The likelihood function $h(q, \lambda)$ for the binary attribute value of one laser of LiDAR is shown in the following equation:

$$h(q,\lambda) = \frac{1}{\sqrt{2\pi\sigma_h^2}} exp\left\{-\frac{(q-\lambda)^2}{2\sigma_h^2}\right\} \tag{2}$$

where λ and q are the measured attribute value and the attribute value obtained from each particle's posture using map information, respectively. σ_h^2 is the variance of the error of the distance value.

Finally, we calculate the weight (i.e., likelihood) ω of each particle by calculating and multiplying the likelihood functions of (1) and (2) for each laser, as shown in the following equation:

$$\omega = \sum_{j=0}^{n} g(p,\mu)h(q,\lambda) \tag{3}$$

where n means the number of lasers. The weights obtained by the likelihood function in (3) is higher if the distance value and the attribute value matched.

III. SIMULATION EXPERIMENT

Simulation experiments were conducted to verify that the proposed method can be used to accurately estimate the pose of a mobile robot in environments with few geometrical features. Using simulated measurement data, pose estimation was performed for both the proposed and reference methods [1], and evaluated by calculating the Euclidean distance from the robot position to the predicted robot position.

A. *Simulation Environments*

In this paper, to verify that the proposed method is effective regardless of the placement of water puddles, simulations were conducted under two different conditions: Simulation *A*, in which water puddles are placed densely in a long corridor, and Simulation *B*, in which water puddles are placed over the entire map. Figures 4 and 5 show the conditions of Simulation *A* and *B*.

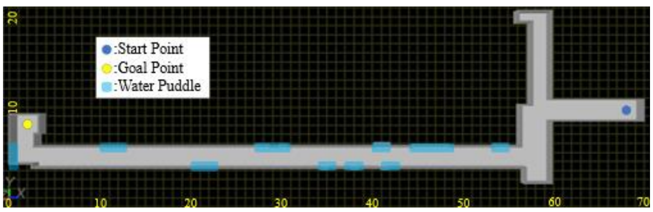

Figure 4. Simulation *A*.

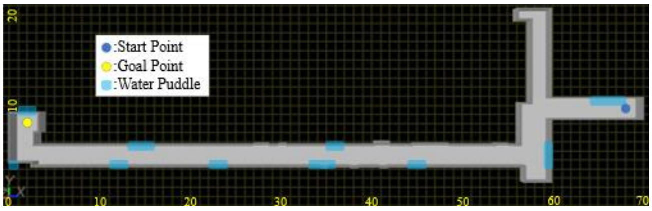

Figure 5. Simulation *B*.

In this simulation, a two-dimensional grid map generated from the shape information of the corridor on the 7th floor of Building No. 2 at the Korakuen Campus of Chuo University was used. The light gray area is a flat floor with a height of 0. Darker gray areas represent walls. Other black areas are assumed to be empty. The size of the entire map is roughly 20 m long and 70 m wide, with one cell of the grid being a square 1 m long and 1 m wide. The coordinate system in the lower left shows the origin. The initial position of the robot was (68 m, 9.5 m) and the goal position was (2 m, 8 m). Ten water puddles were virtually placed in the light blue areas of Figures 4 and 5 in the simulation environment. The attribute values of the water puddle were set to 0 and 1, which are binary values. Here, 0 means a general wall and 1 means a water puddle. The displacement of the odometry was calculated from the simulation results of the robot's autonomous navigation, and a random noise was added to the displacements in the range of -15%-15% to the displacement.

B. Simulation Results

The results of simulation *A* calculated by the proposed and reference methods are shown in Figure 6 and Table 1. The results of simulation *B* in Figure 7 and Table 2. The vertical axis represents the error in Euclidean distance, expressed in meters. The horizontal axis represents frames, and in this simulation, the mobile robot reached the goal in 928 frames. The black line shows the error of the position estimated by the reference method, and the red line shows the error of the position estimated by the proposed method.

The average and maximum values of the position error for all frames for each of the reference and proposed methods are shown in Table 1 for Simulation *A* and Table 2 for Simulation *B*.

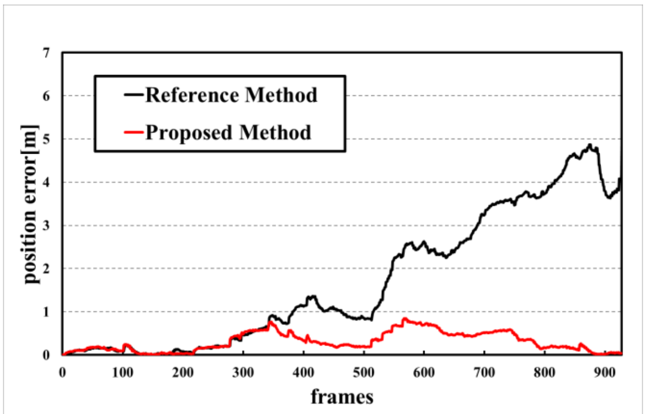

Figure 6. Results for simulation *A*.

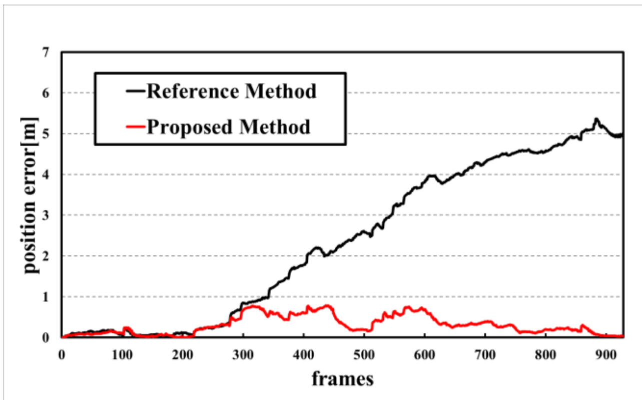

Figure 7. Result of simulation *B*.

TABLE I. ERROR OF SIMULATION *A*

	Simulation *A*	
	Reference method	***Proposed method***
Average [m]	1.69	0.31
Max [m]	4.93	0.85

TABLE II. ERROR OF SIMULATION *B*

	Simulation *B*	
	Reference method	***Proposed method***
Average [m]	2.37	0.31
Max [m]	5.36	0.79

C. Discussion

Figures 6 and 7 and Tables 1 and 2 show that, overall, the errors of the proposed method are smaller than those of the reference method. In both simulations *A* and *B*, 0th-300th frames, the error of the proposed method is almost the same as that of the reference method, and the error is suppressed. On the other hand, 300-928th frames, both simulations *A* and *B* show an increase in error for the reference method and a suppression in error for the proposed method. Therefore, we first consider 0th-300th frames, and then 300-928th frames.

Figure 8 shows the position of the mobile robot in the 300th frame of simulation *A* and its trajectory up to that point. Figure 9 shows the position of the mobile robot in the 300th frame of simulation *B* and its trajectory up to that point.

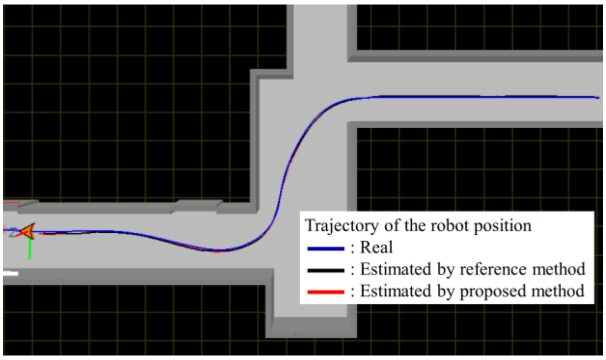

Figure 8. 300th frame of simulation *A*.

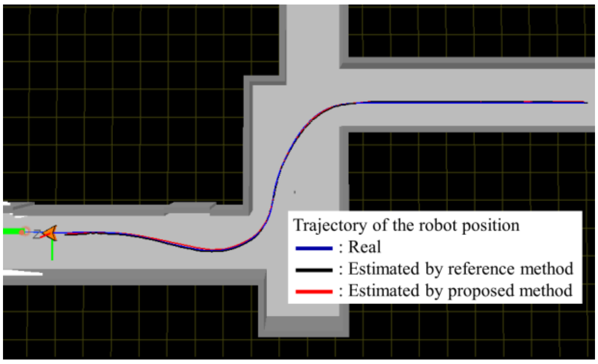

Figure 9. 300th frame of simulation *B*.

The blue line shows the trajectory of the robot autonomous navigation, while the black and red lines represent the trajectory of the robot position estimated by the reference and proposed methods, respectively. In both simulations *A* and *B*, the errors of the reference and proposed methods were almost the same in 0-300th frames. In the autonomous driving in 0-300th frames, there abundant of shape information around the driving path of the mobile robot. Therefore, both the reference method and the proposed method were able to achieve highly accurate pose estimation.

Figure 10 shows the position of the mobile robot in the 928th frame of simulation *A* and its trajectory up to that point. Figure 11 shows the position of the mobile robot in the 928th frame of simulation *B* and its trajectory up to that point.

In the autonomous navigation in the 300-928th frames, the mobile robot navigated a straight corridor of approximately 50 m. The area around the autonomous navigation path by the robot lacks features of shape information, but the attribute values of water puddles are abundant. Therefore, the reference method, which only considers shape information, has a large accumulating error. On the other hand, the proposed method considers not only shape information but also attribute information, so that it can obtain the attribute values of water puddles even in an environment where the shape features are scarce, and thus can reduce the error.

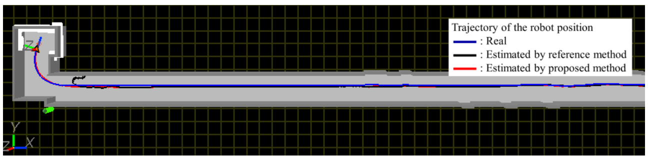

Figure 10. 928th frame of simulation *A*.

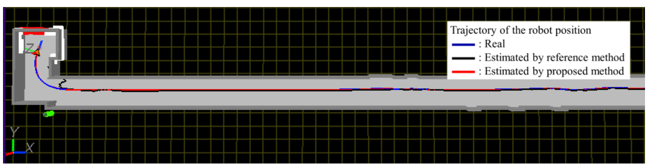

Figure 11. 928th frame of simulation *B*.

IV. Conclusion

In this paper, we proposed a method to improve the accuracy of pose estimation by combining the likelihood of shape information and the likelihood of binary attribute information in water puddles in the likelihood function of particle filters. To verify the superiority of the proposed method, two simulation patterns with different water puddle arrangements were performed, and both showed superior results.

As a future prospect, the accuracy of pose estimation will be verified by conducting autonomous navigation of the robot not in the simulation environment but in a real environment. Furthermore, when driving in a nuclear reactor building after a disaster, the driving surface is expected to be rubble and uneven, and the movement of the mobile robot will be three-dimensional. We will develop a system that can perform highly accurate pose estimation using attribute information even in such an environment.

References

[1] F. Dellaert, D. Fox, W. Burgard and S. Thrun, “Monte Carlo Localization for Mobile Robots,” In Proc. of IEEE ICRA, pp. 1322-1328, 1999.

[2] S. Thrun, D. Fox, W. Burgard and F. Dellaert, “Robust Monte Carlo Localization for Mobile Robots,” Artificial Intelligence, vol. 128, pp. 99-141, 2001.

[3] A. Georgiev and P. K. Allen, “Localization methods for a mobile robot in urban environments,” IEEE Transactions on Robotics, vol. 20, no. 5, pp. 851-864, 2004.

[4] S. M. Umer, Y. Ou and W. Feng, “A novel localization and navigation approach for an indoor autonomous mobile surveillance robot," 2014 4th IEEE International Conference on Information Science and Technology, pp. 5-10, 2014.

[5] K. Ohno, T. Tsubouchi, B. Shigematsu and S. Yuta, “Differential GPS and Odometry-based Outdoor Navigation of a Mobile Robot,” Advanced Robotics, vol. 18, no. 6, pp. 611-635. 2004.

[6] H. Nishimura, J. Meguro, D. Murata, Y. Amano, T. Hashizume, and J. Takiguchi, “Accurate GPS Positioning Using Infrared Full-Surround Camera,” GPS/GNSS Symposium, vol. 2006, pp. 133-139, 2006. (in Japanese)

[7] I. Yamaguchi, N. Furushiro, T. Ando, H. Furusei, and T. Yanagi, “Development of robust self-positioning technique using a front-surrounding fisheye camera,” Transactions of Society of Automotive Engineers of Japan, vol. 45, no. 3, pp. 597-602, 2014.

[8] R. Hatakeyama, O. Kanai, and H. Date, “GPU Programming for Fast Indoor Self-Position Estimation Using a Depth Camera,” Proc. Japan Society for Precision Engineering, 2014, pp. 391-392, 2014. (in Japanese)

[9] J. Folkesson and H. I. Christensen, “Closing the Loop with Graphical SLAM,” IEEE Transactions on Robotics, Vol. 23, No. 4, pp. 731-41, 2007.

[10] R. Kataoka, I. Tadokoro, Y. Ji, H. Fujii, H. Kono and K. Umeda, "Performance Improvement of SLAM based on global registration using LiDAR Intensity and Measurement Data of Puddle," 2021 18th International Conference on Ubiquitous Robots (UR), pp. 553-556, 2021.

[11] M. Sugawara, H. Fujii, H. Kono, and Y. Ji, “3D visualization of near-infrared information for construction of water source survey map using teleoperated robot,” Proc. 20th SICE Conference on System Integration (SI2019), 2019. (in Japanese)